JOURNAL OF THERMOPHYSICS AND HEAT TRANSFER
Vol. 16, No. 1, January–March 2002

Novel Pressure-Sensitive Paint for Cryogenic and Unsteady Wind-Tunnel Testing

Keisuke Asai,* Yutaka Amao,† and Yoshimi Iijima‡
National Aerospace Laboratory, Tokyo 182-8255, Japan
Ichiro Okura§
Tokyo Institute of Technology, Kanagawa 226-8501, Japan
and
Hiroyuki Nishide¶
Waseda University, Tokyo 169-8555, Japan

A novel pressure-sensitive paint (PSP) formulation suitable for use in cryogenic and unsteady wind-tunnel testing has been developed. This new PSP uses poly [1–(trimethylsilyl)–1–propyne] [poly(TMSP)] as a binder. Poly(TMSP) is a glassy polymer having extremely high gas permeability. Unlike the conventional polymer-based paints, PSP based on poly(TMSP) maintains oxygen sensitivity even at cryogenic temperatures and exhibits fast response time. This paint is sprayable on any model surface including stainless steel and ceramics. These capabilities allow us to apply this PSP to a cryogenic wind tunnel and a short-duration shock tunnel. To demonstrate the capability of poly(TMSP)-PSP for pressure measurements in a cryogenic wind tunnel, a circular-arc bump model and a delta wing model were tested in the National Aerospace Laboratory 0.1-m Cryogenic Wind Tunnel at 100 K. It has been verified that poly(TMSP)-PSP can provide high *S/N* pressure distribution data at high O_2 concentration. A comparison of the measured intensity data with the pressure tap measurements has suggested that the in situ calibration can be used to obtain quantitative pressure data. It was also demonstrated that poly(TMSP)-PSP could visualize the complex flowfield on a stainless steel delta wing, including primary and secondary separation vortices and their breakdown.

Nomenclature

A, B = calibration coefficients of Stern–Volmer equation, $I_{\text{ref}}/I = A + B(P/P_{\text{ref}})$
b = local wing span, m
C_p = pressure coefficient, $(P - P_\infty)/q_\infty$
c = chord length, m
D = mass diffusivity of polymer, Table 1
I = luminescent intensity, counts
M = Mach number
$[O_2]$ = oxygen concentration, ppm
P = pressure, kPa
P_G = gas permeability of polymer, Table 1
q = dynamic pressure, kPa
S = solubility of polymer, Table 1
T = temperature, K
T_G = glass transition temperature, K
x = chordwise location, m
y = spanwise location, m
τ = time constant to a step change in pressure, second

Subscripts

ref = reference
t = stagnation
∞ = freestream

Presented as Paper 2000-2527 at the AIAA 21st Aerodynamic Measurement Technology and Ground Testing Conference, Denver, CO, 19–22 June 2000; received 26 February 2001; revision received 12 July 2001; accepted for publication 12 July 2001.

*Group Leader, Advanced Measurement Technology Group, Fluid Science Research Center, 7-44-1 Jindaiji-Higashi, Chofu; asai@nal.go.jp. Associate Fellow AIAA.

†Research Scientist, Advanced Measurement Technology Group, Fluid Science Research Center, 7-44-1 Jindaiji-Higashi, Chofu; currently Lecturer, Department of Applied Chemistry, Oita University, 700 Dannoharu, Oita.

‡Research Engineer, Advanced Measurement Technology Group, Fluid Science Research Center, 7-44-1 Jingdaiji-Higashi, Chofu.

§Professor, Department of Biotechnology, 4259 Nagatsuda, Midori-ku, Yokohama.

¶Professor, Department of Polymer Chemistry, 3-4-1 Okubo, Shinjuku-ku.

Introduction

USE of pressure-sensitive paint (PSP) is an innovative optical surface measurement technique in the aerospace community.[1,2] Using PSP, one can obtain a complete surface pressure map on model surfaces without using pressure taps and transducers. Currently, PSP has been applied to aircraft and rocket development wind-tunnel tests and has been very useful in eliminating considerable cost and time required for the tests.

In parallel with this practical work, effort has been made to improve current PSP formulations. Usually, PSP is composed of probe molecules (porphyrin, ruthenium complexes, pyrene, etc.) and a polymer binder [GP197, RTV, FIB, poly(IBM–co–TFEM), etc.]. These polymer-based PSPs, however, still have several deficiencies such as 1) pressure measurement error due to temperature dependence of PSP, 2) slow response to a rapid change in pressure, and 3) oxygen sensitivity loss at low temperatures. Note that these problems are attributed not only to the properties of the probe molecules but also to those of the binder material.

In theory, luminescence quenching by oxygen is expressed by the well-known Stern–Volmer equation. Liu et al.[3] have derived an approximate expression of Stern–Volmer relationship and found that a polymer having low activation energy for oxygen diffusion should have lower temperature sensitivity. Experimental work by Schanze, et al.[4] has also indicated that oxygen diffusivity of the binder is the most important factor determining temperature effects on PSP.

The time response of PSP to a pressure change is also dependent on polymer binder properties.[5–7] For example, a first-generation paint such as platinum octaethylporphyrin (PtOEP)/GP197 has a very slow time response (on the order of seconds). This is attributed

Table 1 Comparison of poly(TMSP) and poly(DMS) properties[17]

Polymer	O_2 permeability, $cm^3(STP)\ cm \times 10^{10}$ $cm^2 s\ cm\ Hg$	Diffusion coefficient, $cm^2/s \times 10^6$	Solubility, $cm^3(STP) \times 10^4$ $cm^3\ cm\ Hg$	Glass transition temperature, °C
Poly(DMS)	960(at 35°C)	40(at 35°C)	24(at 35°C)	−127
Poly(TMSP)	7700(at 30°C)	47(at 30°C)	170(at 30°C)	>200

to low gas diffusivity in the polymer layer. Previous studies on the time response of PSP have shown that time constant τ to a step change in pressure is proportional to the square of the PSP film thickness and inversely proportional to the mass diffusivity of the polymer binder. This relationship suggests that fast responding PSP requires a polymer binder with high oxygen diffusivity.

Considerable effort has been made to develop a PSP working at cryogenic temperatures. The development of cryogenic PSPs was initiated by the need for a global pressure measurement technique for high Reynolds number tests in a cryogenic wind tunnel. To date, three types of cryogenic PSPs have been reported. All of these cryogenic paints use some kinds of porous material as a binder.

Asai,[8] Asai et al.,[9] and Erausquin et al.[10] first developed a cryogenic PSP based on anodized aluminum. In this coating, probe molecules such as $Ru(dpp)_3$ are directly deposited on an anodized surface by an electrochemical process. Sakaue et al.[11] modified the process to make an anodized coating with improved sensitivity and stability. These anodized-aluminum- (AA-) PSPs have been successfully used to measure the surface pressure distributions on a 14%-thick circular arc bump model in the National Aerospace Laboratory (NAL) 0.1-m Cryogenic Wind Tunnel.

Jordan et al.[12] have developed a sol–gel-based PSP for wind tunnel tests. It is reported that this coating keeps pressure sensitivity even at 150 K. Recently, Upchurch et al.[13] developed a polymer-based cryogenic PSP that is universally applicable to all types of models including stainless steel. This paint has been successfully demonstrated for pressure measurements on an airfoil in the 0.3-m cryogenic wind tunnel at NASA Langley Research Tunnel, but the formulation of this paint is not open.

In general, a cryogenic PSP exhibits fast time response because it is based on a porous binder. Recently, Sakaue and Sullivan[14] measured the time response of AA-PSP using a shock tube apparatus. Their study indicates that AA-PSP has a time response of 30–100 μs. Similar results were obtained by Teduka et al.[15] in a pressure jump apparatus using a fast opening solenoid valve. Nakakita et al.[16] have successfully demonstrated the capability of AA-PSP for pressure measurements on a model in a short-duration Mach 10 shock tunnel with the duration time of 20 ms.

The purpose of this paper is to present a new PSP formulation that can be applied to a cryogenic wind tunnel and a short-duration shock tunnel. A polymer, poly[1–(trimethylsilyl)–1–propyne] [poly(TMSP)], is used as a binder that has extremely high gas permeability. Note that this PSP can be dissolved in solvent and applied using an airbrush to any model surfaces including stainless steel. This is in contrast to AA-PSP that is applicable only to aluminum or aluminum alloy.

In this paper, the results from sample tests of poly(TMSP)-based PSP (pressure and temperature sensitivity, time response, low-temperature characteristics, etc.) are presented. The potential of the new paint for cryogenic and unsteady wind-tunnel testing is discussed by comparing poly(TMSP)-based PSP and AA-PSP data. To validate the cryogenic performance of poly(TMSP)-PSP, tests with a circular-arc bump model and a delta wing model were conducted in the 0.1-m Transonic Cryogenic Wind Tunnel at the NAL. From a comparison between the paint-derived pressure distribution data and conventional tap measurements, the paint calibration procedures and the measurement accuracy are evaluated. PSP images obtained for a delta wing model will be also presented to demonstrate the capability of the new PSP to visualize the complex flowfield.

New PSP Formulation

Poly(TMSP) is a high molecular-weight polymer that was first synthesized by Toshio Masuda of Kyoto University in Japan.[17] It is glassy material with a large free volume, having a low diffusion barrier to oxygen and, hence, high oxygen permeability.

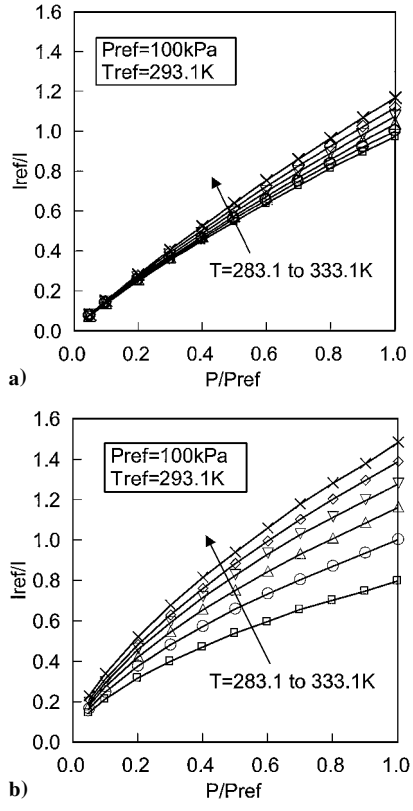

Fig. 1 Stern–Volmer plots for a) poly(TMSP)-PSP and b) AA-PSP.

The properties of poly(TMSP) are listed in Table 1. Those for poly(dimethylsiloxane) [poly(DMS)], common binder in the current PSP, for example, GP197, are also shown in Table 1 for comparison. As is seen, the diffusion coefficient D of poly(TMSP) is comparable to that of poly(DMS), but this value is extremely high compared with other glassy polymers. On the other hand, the solubility S of poly(TMSP) is seven times higher than that of poly(DMS). As a result, the permeability, $P_G = SD$, of poly(TMSP) to oxygen is greater than poly(DMS) approximately by a factor of eight. Note that poly(TMSP) has the highest permeability at present.

We use poly(TMSP) as a binder for a high-performance PSP.[18] This new PSP can be dissolved in a common solvent like toluene and then applied on any model surface, for example, stainless steel, using a standard airbrush. In this study, we used PtOEP as probe molecules. PSP samples were prepared by casting PSP on a glass plate or applying PSP on an aluminum plate using an airbrush. For wind-tunnel tests, PSP was sprayed directly onto model surfaces using an airbrush, and no undercoat was applied. The thickness of the PSP coating was approximately 2 μm. The surface roughness measured by a stylus device was 0.18 μm.

Sample Tests

Static Calibration

Figure 1 shows Stern–Volmer plots of luminescent intensity and pressure for poly(TMSP) paint and AA-PSP. These data were obtained in a pressure chamber with a Peltier thermocontroller inside. The pressure was varied from 5 to 100 kPa while the temperature ranges from 10 to 60°C. A xenon lamp excited the sample, and a

cooled charge-coupled device (CCD) camera detected the emission from the samples. For poly(TMSP) paint, bandpass filters centered at 400 and 650 nm were used for excitation and emission, respectively. The accuracy of the reference pressure sensor was 0.05% of the full-scale value (0.25 kPa). We also monitored the intensity of excitation light using a photodiode. The total uncertainty caused by these factors is much smaller than the symbol size in the figures.

As shown in Fig. 1, the new PSP has higher pressure sensitivity than AA-PSP. The slope of the Stern–Volmer curve [B in $I_{\mathrm{ref}}/I = A + B(P/P_{\mathrm{ref}})$] at 293 K (20°C) is as high as 0.95. This high quenching constant for oxygen makes this coating suitable for applications to low-pressure measurements around 5 kPa. Note that the new coating is much less dependent on temperature than AA-PSP. The temperature sensitivity of poly(TMSP) paint, $\Delta(I/I_{\mathrm{ref}})/\Delta T$, at 20°C (293 K) is about −0.4%/°C, one-third that for AA-PSP (−1.4%/°C). This greatly improves the accuracy in pressure measurements, especially in unsteady tests in which temperature effects must be corrected in real time.

Time Response

The time-response tests of the poly(TMSP) paint were carried out using a pressure jump apparatus shown in Fig. 2. This apparatus is constructed around a small-volume test chamber that is connected directly to a fast opening valve having a time constant of a few milliseconds. We used a Kuliter® pressure transducer as a reference. The accuracy of this sensor was 0.1% of the full-scale value, and the resonance frequency was 300 kHz. Sample plates used in this test were aluminum coupons coated with PSP.

Figure 3 shows the time response of luminescent intensity for various paints to a step change in pressure from vacuum to 1 atm.

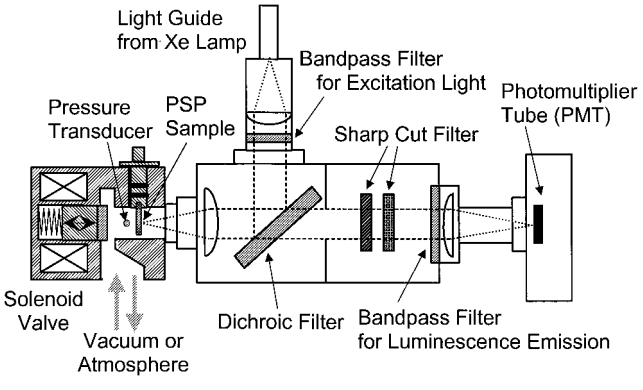

Fig. 2 Schematic of pressure jump apparatus.

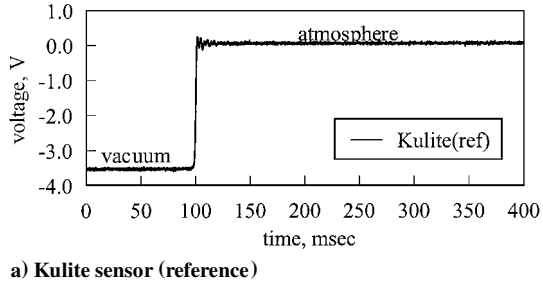

a) Kulite sensor (reference)

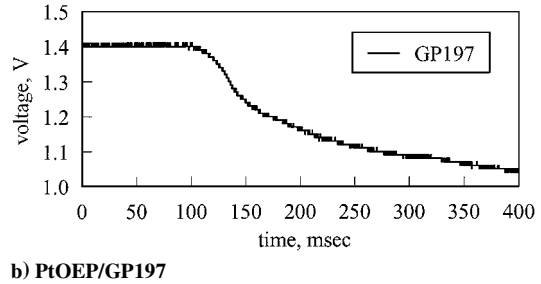

b) PtOEP/GP197

Figures 3a–3d show data for the reference sensor, GP197, AA-PSP, and poly(TMSP), respectively.

It is seen that GP197-based PSP is very slow, and its time constant is on the order of several seconds. In contrast, AA-PSP has submillisecond time response as previously reported.[14,15] The response of poly(TMSP)-PSP is a little bit slower than AA-PSP but much faster than conventional polymer-based paints. The time constant of poly(TMSP)-PSP is about a few milliseconds. This value is sufficiently small for use in a shock tunnel where the test duration is several to tens of milliseconds.[16]

Cryogenic Calibration

Calibration tests of PSP samples at cryogenic temperatures were carried out in the test section of the NAL 0.1-m Cryogenic Transonic Wind Tunnel (see the next section for details). The aluminum plate coated with poly(TMSP) paint was mounted on the test section sidewall, and luminescence from the sample was detected through the observation window. The oxygen concentration of tunnel working gas was controlled by blowing dry air in the tunnel.

Figure 4 shows the luminescence intensity variation with oxygen concentration for poly(TMSP) and its Stern–Volmer plot for $T = 100$ K. The data for AA-PSP are also shown for comparison. The temperature was set at 100 K, while the stagnation pressure was 190 kPa. The oxygen concentration ranged from near zero (5 ppm) to 1000 ppm. The scatter shown in Fig. 4 was caused by the uncertainty in a ZrO_2 oxygen sensor to monitor oxygen concentration in the flow (2% of the reading). The other sources of error such as errors from the camera shot noise were much smaller.

As shown clearly in Fig. 4, poly(TMSP) maintains high sensitivity to oxygen over a wide range of oxygen concentrations. On

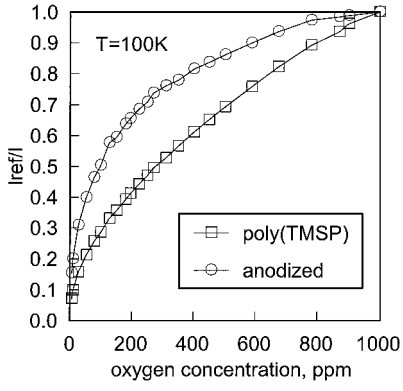

Fig. 4 Quenching characteristics of poly(TMSP)-PSP and AA-PSP at 100 K.

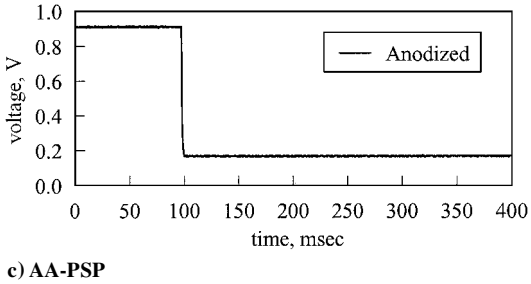

c) AA-PSP

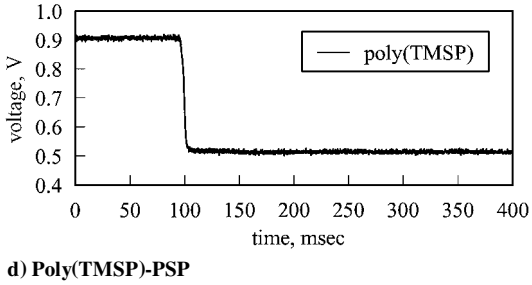

d) Poly(TMSP)-PSP

Fig. 3 Time response of various PSPs to a step change in pressure.

the other hand, AA-PSP exhibits a highly nonlinear Stern–Volmer curve, and its oxygen sensitivity decreases with increasing oxygen concentration. Testing at higher oxygen concentration is advantageous in terms of the signal-to-noise ratio because a spatial variation in oxygen over the model surface becomes larger as the oxygen concentration is increased. This indicates that poly(TMSP)-PSP is superior to AA-PSP from the accuracy point of view.

Description of Experiments: Verification Tests in a Cryogenic Wind Tunnel

Facility

To demonstrate the capability of poly(TMSP)-PSP for pressure measurement in a cryogenic wind tunnel, a series of experiments were conducted in the NAL 0.1-m Transonic Cryogenic Wind Tunnel (TCWT). This facility is a closed-circuit, fan-driven wind tunnel operated with cryogenic nitrogen as the working gas. The minimum flow temperature is 90 K with stagnation pressure ranging from 110 to 200 kPa. The test section is 0.1×0.1 m and is equipped with slotted top and bottom walls of 4% porosity and solid sidewalls. To prevent light from reflecting on the wall, the inside of the test section was anodized in black.

Figure 5 shows a schematic diagram of experimental setup in the NAL 0.1-m TCWT. The tunnel is operated by controlling both liquid nitrogen injection and gaseous nitrogen exhaust. Oxygen gas was injected through a strut located just downstream of the test section. A small amount of exhaust gas is sampled and fed into a zirconia (ZrO_2) sensor to monitor the oxygen concentration in flow. The oxygen concentration was varied from near zero to 2000 ppm by adjusting the flow rate of injected air.

Models

In the present study, we used two different models for verification purposes. One is a two-dimensional bump model (Fig. 6) and other is a clipped delta wing (Fig. 7). The bump model cross section is a 14% circular arc, and the chord length is 50 mm. This model is made of aluminum and consists of one center strip having 16 static pressure taps and 4 removable strips 8 mm in width. Two strips were coated with poly(TMSP)-PSP using an airbrush. The other two strips were anodized using the Sakaue et al. method (AA-PSP).[11] In this experiment, Mach number was set at either 0.4 or 0.82. The temperature and the pressure were maintained at 100 K and 190 kPa, respectively. The oxygen concentration was varied up to 1000 ppm.

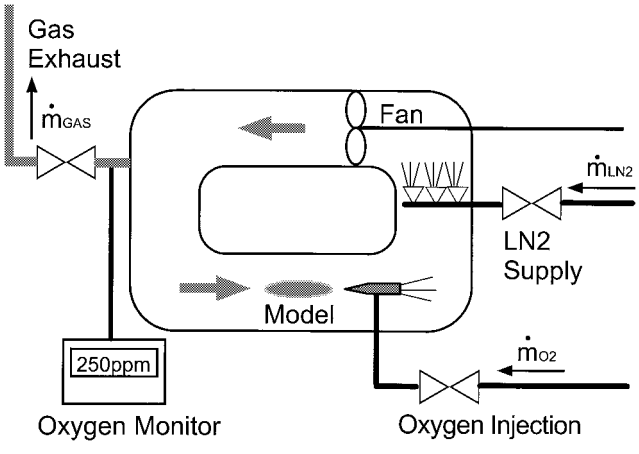

Fig. 5 Schematic diagram of experimental setup at the NAL 0.1-m TCWT.

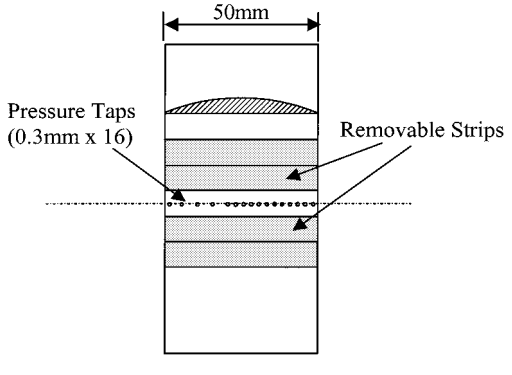

Fig. 6 Aluminum 14%-thick circular-arc bump model.

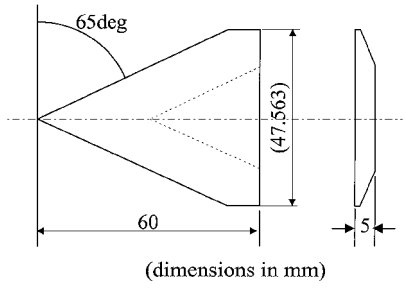

Fig. 7 Stainless steel 65-deg sweep delta wing with sharp leading edge.

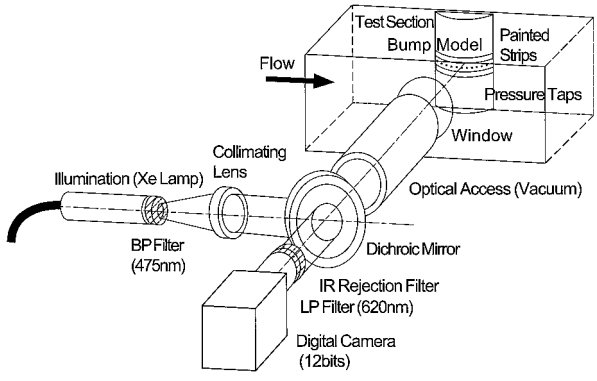

Fig. 8 Schematic of the optical measurement system for the NAL 0.1-m TCWT tests.

The delta wing model has a 65-deg sweep angle and a sharp leading edge. The planform of this model is the same as that of the well-known Euler model. The model chord length c is 60 mm and eight pressure taps were located on the portside wing at $x/c = 80\%$. The model was strut mounted on the sidewall at an angle of attack of 20 deg. This model is made of stainless steel (SUS304), and poly(TMSP)-PSP was applied using a standard airbrush.

Optical Equipment

Figure 8 is a schematic of the optical setup. The model was mounted on the sidewall, and optical access was gained through a 70-mm-diam observation window on the opposite sidewall. We used a 300-W xenon lamp with a bandpass filter (400 ± 50 nm) for excitation light. A dichroic mirror (550 nm) was used to separate paint emission from excitation light. The emission from the coating was detected by a cooled CCD digital camera with 14-bit intensity resolution. A bandpass filter (650 ± 20 nm) was placed in front of the camera lens.

Data Reduction

The images acquired by the digital camera were processed using MATLAB®. To cancel the undesirable effects of spatial nonuniformities in illumination and coating thickness, we took the ratio of luminescent intensity I with respect to the intensity at a reference condition, I_{ref}.

In conventional wind tunnels, an image taken at a no-wind condition is usually used as the reference. Note, however, that a wind-off (still) condition cannot be attained in a cryogenic wind tunnel because the tunnel is being operated by a continuous injection of liquid nitrogen. Therefore we use an image taken at low speeds, for example, Mach 0.1, as an alternative reference, where the dynamic pressure is so small that distribution of oxygen concentration over the model surface can be neglected. In this particular experiment, an image taken at Mach 0.4 was used as the reference. This is the lowest

Mach number at which the tunnel can keep stable operation. A variation of oxygen concentration on the model cannot be neglected at this Mach number. Thus, we assumed here that the pressure distribution at $M = 0.4$ was known to be constant. This assumption does not contain any approximation, but paint calibration results are valid only when they are applied pixel by pixel.

To calculate pressure from measured intensity ratio, we have to determine the paint calibration coefficients by experiment. There are two calibration approaches, in situ and a priori.

The in situ method is performed during the run condition on a model equipped with pressure taps, by fitting the luminescent intensity data and the pressure tap data at spatially corresponding locations. The isothermal assumption is valid because a variation in model surface temperature is negligible in a cryogenic wind tunnel. This means we can apply the coefficients obtained locally by the in situ method to entire model surfaces.

The a priori method is a calibration procedure without using any pressure taps. The a priori method is usually performed in a calibration chamber on a sample plate coated with the same paint as applied on the model. The a priori calibration also can be carried out in a tunnel by changing oxygen concentration in the flow. Using this approach, a calibration of PSP coating on the model surface can be performed pixel by pixel. The a priori calibration is desirable because no pressure tap measurements are required.

Results and Discussion

Bump Model Test

Figure 9 shows the luminescence intensity profiles of poly(TMSP)-PSP at two different Mach numbers, $M = 0.4$ and 0.82. Both data were taken at the same temperature ($T_t = 100$ K) and oxygen mole fraction ($[O_2] = 1000$ ppm). The difference between the two intensities is about 20% of the reference value.

Figure 10 is a plot of the ratio of the Mach 0.82 image with the Mach 0.40 reference image. It is evident that the intensity ratio is

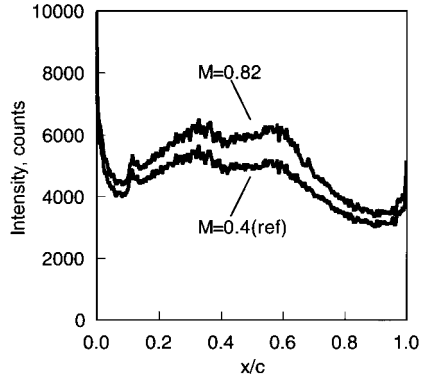

Fig. 9 Luminescent intensity profiles of poly(TMSP)-PSP for Mach 0.40 and 0.82, $T_t = 100$ K and $[O_2] = 1000$ ppm.

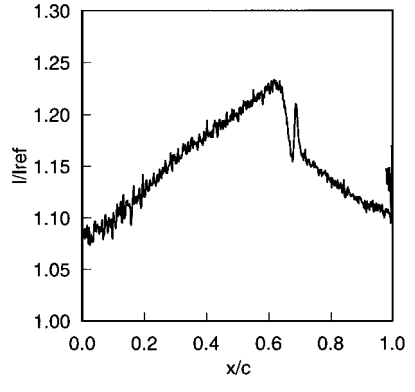

Fig. 10 Luminescent intensity ratio of high-speed and low-speed (reference) images.

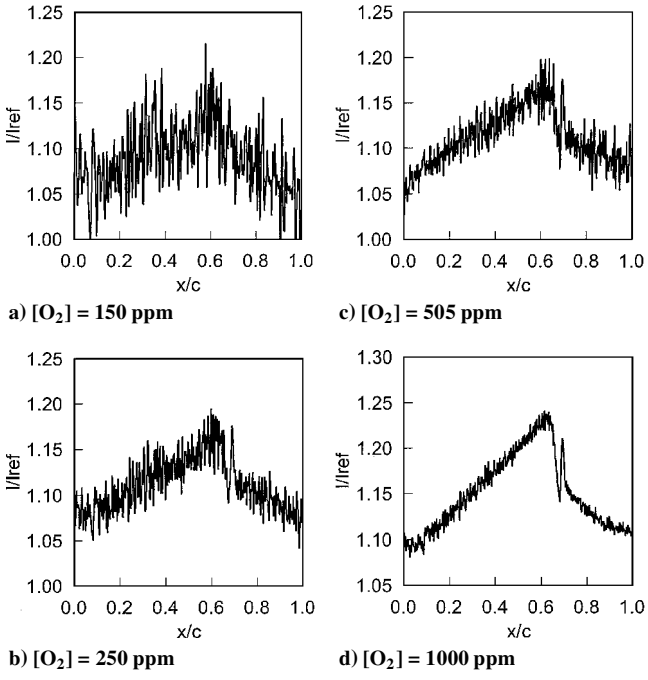

Fig. 11 Effects of oxygen concentration in flow on the signal-to-noise ratio of intensity ratio data.

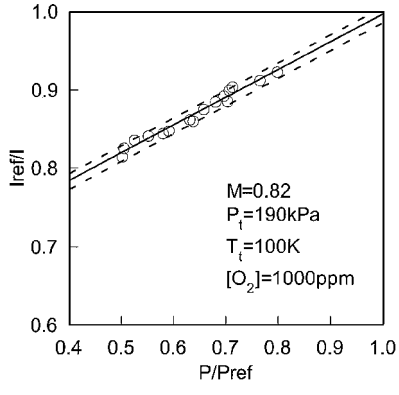

Fig. 12 In situ calibration curve of poly(TMSP)-PSP for the case of $[O_2] = 1000$ ppm.

representing a chordwise variation in surface pressure on a typical transonic airfoil. Flow accelerates from the leading edge to the maximum-thickness position and causes an abrupt pressure jump due to shock at about $x/c = 0.65$. Pressure did not recover at the trailing edge due to the occurrence of shock-induced separation. A pair of intensity spikes observed at the foot of a shock wave is not a real pressure change, but a shadow of a shock wave projected onto the model surface by excitation light (same as shadowgraph).

Figures 11a–11d show the intensity ratio images taken for $[O_2] = 150$, 250, 505, and 1000 ppm, respectively. Note that the spatial noise dramatically reduces as the oxygen concentration is increased. As already discussed, this is because poly(TMSP)-PSP maintains oxygen sensitivity at higher oxygen concentrations. The optimal oxygen concentration should be determined by tradeoff between a loss in luminescent intensity and a gain in oxygen concentration.

Figure 12 is a plot of measured intensity ratio vs pressure tap measurements (in situ calibration). A least-squire fit (solid line) as well as the error bands (2σ, broken lines) are also shown in Fig. 12. As is evident, the relation between I_{ref}/I and P/P_{ref} is practically linear. Also noted is that the calibration curve passes through the point (1,1) as suggested by the Stern–Volmer relation. From these results, it is confirmed that the model surface is fairly isothermal in a cryogenic flow, and we can use a single calibration curve for the entire surface of the model.

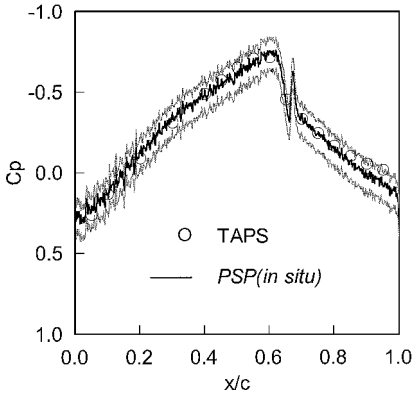

Fig. 13 Pressure distribution reconstructed from PSP data and an in situ method, compared with pressure tap measurements.

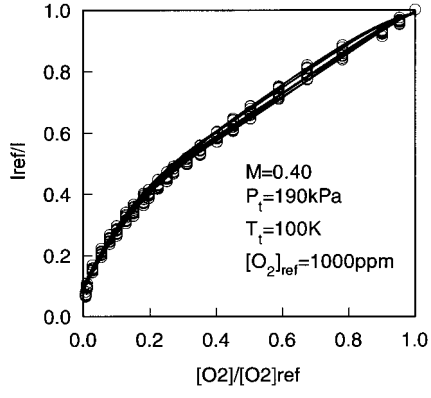

Fig. 14 A priori calibration curve of poly(TMSP)-PSP for 18 different chordwise positions from *x/c* = 5 to 95%.

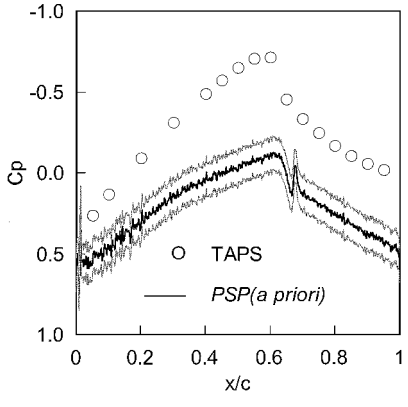

Fig. 15 Pressure distribution reconstructed from PSP data and an a priori method, compared with pressure tap measurements.

Figure 13 is pressure data converted from I_{ref}/I using the calibration line in Fig. 12. The main source of error comes from errors in the calibration. Other sources such as camera shot noise and image registration error are much smaller. The uncertainty of PSP data was estimated from the calibration line and is shown by gray lines. It is seen that PSP-derived data are in excellent agreement with pressure tap measurements except for a small difference in the separated flow region. From these results, it is confirmed that we could employ the in situ calibration for more complicated aircraft configurations and using a smaller number of taps.

Figure 14 shows luminescence intensity variation with oxygen for 18 different chordwise positions from $x/c = 5$ to 95% at low-speed condition (a priori calibration). It is seen that the calibration curve is almost the same for different locations. A fourth polynomial fit was sufficient to provide an accurate description of each curve.

Figure 15 is the pressure distribution obtained using the a priori calibration curve in Fig. 14 on a pixel-by-pixel basis. The uncertainty of PSP data was estimated from the calibration line and is shown by gray lines in Fig. 15. The main source of error comes from the accuracy of a ZiO_2 sensor to monitor oxygen concentration (2% of the reading in the low oxygen concentration range). This introduces errors in calibrating PSP by changing oxygen concentration and in matching the mol fraction of oxygen between low-speed and high-speed flow conditions.

Note, in Fig. 15, that the a priori calibration data did not agree with pressure tap data. Comparing the calibration curves in Figs. 12 and 14, one notices that the slope of the a priori calibration curve is twice as large as that for the in situ curve. This difference causes a significant change in pressure level. The similar results were also reported for AA-PSP.[9–11] This error might be related to unknown phenomena such as adsorption of oxygen and nitrogen gases at cryogenic temperatures. Further study is required to fully understand the underlying physics.

Delta Wing Model Test

The image processing sequence for the delta wing model test is the same as that for the bump model test. Figure 16 shows the raw images (Figs. 16a and 16b) taken at two different Mach numbers ($M = 0.4$ and 0.75) and at the same temperature ($T_t = 100$ K) and oxygen mole fraction ($[O_2] = 997$ ppm). These intensity images show poor spatial uniformity because no optical undercoat was applied on the model in this experiment.

Figure 17 shows the ratio of the high-speed image and the low-speed reference image. It is evident that the effects of nonuniformity of paint thickness were factored out by the ratioing process, and the complex flow structures including leading-edge separation vortices were clearly visualized.

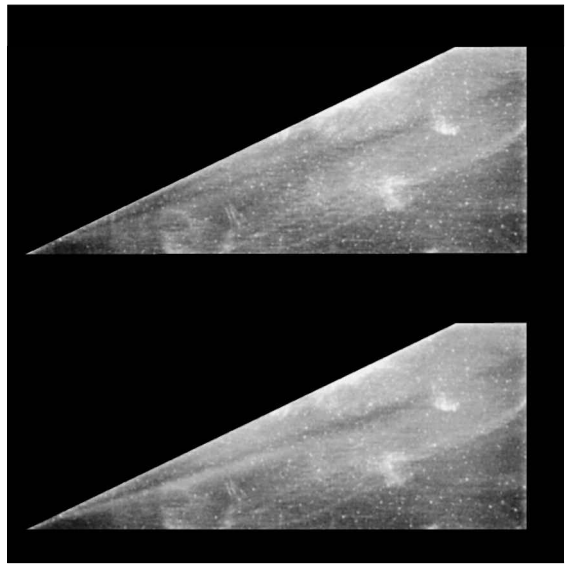

Fig. 16 Raw intensity images for delta wing model tests, a) $M = 0.40$ (ref) and b) $M = 0.75$.

Fig. 17 Processed image for delta wing model, $M = 0.75$, $T_t = 100$ K, $P_t = 190$ kPa, and $[O_2] = 997$ ppm.

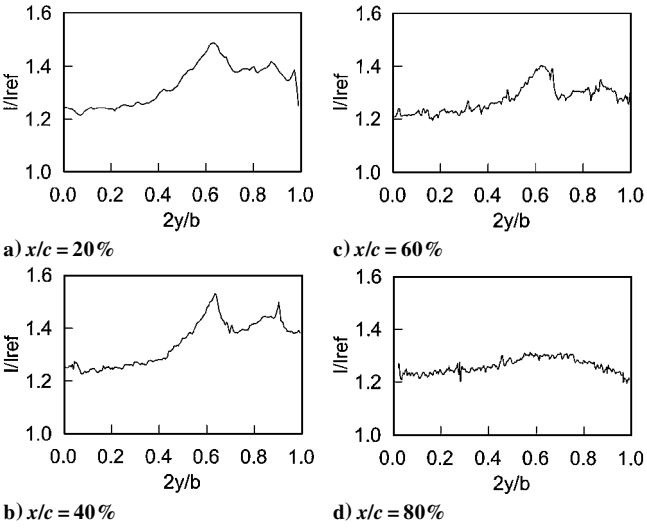

Fig. 18 Spanwise intensity-ratio distributions at different chordwise positions.

Variations of spanwise I/I_{ref} distributions with respect to chordwise location are shown in Fig. 18. Evidently, these profile data represent a typical evolution of leading-edge separation vortices on a delta wing. The primary and secondary separations are clearly seen at $x/c = 20$ and 40%. The secondary vortex starts to burst at $x/c = 60\%$, and the both vortices are completely broken down at $x/c = 80\%$. These intensity plots have a fairly large spatial noise probably because there was not sufficient intensity change between Mach 0.4 and 0.75 images. We plan to conduct more tests with optimized test parameters to evaluate the accuracy of poly(TMSP) paint.

Conclusions

A novel PSP formulation for cryogenic and unsteady tests has been developed. This new paint is based on poly(TMSP), a high polymer with an extremely high diffusion coefficient. This PSP is sprayable on model surfaces using an airbrush and is suitable for three-dimensional models with complicated configurations. Unlike the conventional polymer-based PSPs, poly(TMSP)-PSP works even at cryogenic temperatures and exhibits very fast response time. In this study, the properties of poly(TMSP)-PSP were examined by sample tests as well as wind-tunnel tests in NAL 0.1-m TCWT. The results obtained can be summarized as follows.

1) Poly(TMSP)-based PSP has a higher pressure sensitivity and a lower temperature sensitivity than conventional polymer-based PSPs. Because of its high quenching constant, this coating is most suitable for use in the low-pressure range.

2) The response time for a step change in pressure from vacuum to atmosphere is a few milliseconds. This coating can be applied to short-duration tests in a shock tunnel.

3) Poly(TMSP)-based PSP has an extremely high oxygen sensitivity at cryogenic temperatures. Poly(TMSP) PSP maintains high sensitivity to oxygen over a wide range of oxygen concentrations. This is in contrast to AA-PSP, which loses its sensitivity to oxygen as oxygen concentration increases.

4) When poly(TMSP)-PSP was used, surface pressure distributions over the circular-arc bump model were clearly imaged in a cryogenic wind tunnel. It was shown that poly(TMSP)-PSP could provide high signal-to-noise pressure distribution data at an oxygen concentration of 1000 ppm.

5) It is demonstrated that poly(TMSP)-PSP works on a stainless steel three-dimensional model. The complex flowfield on a clipped delta wing model has been clearly visualized, including primary and secondary separation vortices and their breakdown.

6) The in situ calibration works in a cryogenic wind tunnel. The measured intensity ratio and pressure tap measurements can be fit on a single straight line. On the other hand, there still exist unknown problems with the a priori calibration. Further study is required to attain absolute pressure accuracy.

Acknowledgments

This work is partially supported by Molecular Sensors for Aero-Thermodynamic Research, the Special Coordination Funds of Ministry of Education, Culture, Sports, Science and Technology, Japan. The authors wish to thank Norikazu Teduka, Tokyo University of Agriculture and Technolgy, for his help in calibrating anodized-aluminum pressure-sensitive paint samples. The authors would also like to thank Yasuhiro Egami of the National Aerospace Laboratory for his help in image processing of delta wing test results.

References

[1]Liu, T., Campbell, B. T., Burns, S. P., and Sullivan, J. P., "Temperature and Pressure-Sensitive Luminescent Paints in Aerodynamics," *Applied Mechanics Review*, Vol. 50, No. 4, 1997, pp. 227–246.

[2]Bell, J. H., Schairer, E. T., Hand, L. A., and Mehta, R. D., "Surface Pressure Measurements Using Luminescent Coatings," *Annual Review in Fluid Dynamics*, Vol. 33, Jan. 2001, pp. 1–62.

[3]Liu, T., Guille, M., and Sullivan, J. P., "Accuracy of Pressure-Sensitive Paints," *AIAA Journal*, Vol. 39, No. 1, 2001, pp. 103–112.

[4]Schanze, K. S., Carroll, B. F., Korotkevitch, S., and Morris, M. J., "Temperature Dependence of Pressure-Sensitive Paints," *AIAA Journal*, Vol. 35, No. 2, 1997, pp. 306–310.

[5]Baron, A. E., Danielson, J. D., Gouterman, M., Wan, J., and Callis, J. B., "Submillisecond Response Times of Oxygen-Quenching Luminescent Coatings," *Review of Scientific Instrumentations*, Vol. 64, No. 12, 1993, pp. 3394–3402.

[6]Carroll, B. F., Abbitt, J. D., Lukas, E. W., and Morris, M. J., "Step Response of Pressure-Sensitive Paints," *AIAA Journal*, Vol. 34, No. 3, 1996, pp. 521–526.

[7]Fonov, S., Mosharov, V., Radchenko, V., Engler, R. H., and Klein, C., "Application of the PSP Investigation of the Oscillating Pressure Fields," AIAA Paper 98-2503, June 1998.

[8]Asai, K., "Luminescent Coating with an Extremely High Oxygen Sensitivity at Low Temperatures," Patent Pending, No. H9-207351, July 1997, Japan.

[9]Asai, K., Kanda, H., Cunningham, C., Erausquin, R., and Sullivan, J. P., "Surface Pressure Measurement in a Cryogenic Wind Tunnel by Using Luminescent Coating," *Proceedings of the 17th International Congress on Instrumentation in Aerospace Simulation Facilities (ICIASF)*, Inst. of Electrical and Electronics Engineers, New York, 1997, pp. 105–114.

[10]Erausquin, R., Cunningham, C., Sullivan, J. P., Asai, K., Kanda, H., and Kunimasu, T., "Cryogenic Pressure Sensitive Fluorescent Paint Systems," AIAA Paper 98-0588, Jan. 1998.

[11]Sakaue, H., Sullivan, J. P., Asai, K., Iijima, Y., and Kunimasu, T., "Anodized Aluminum Pressure Sensitive Paint in Cryogenic Wind Tunnels," *Proceedings of the 45th International Instrumentation Symposium*, Instrument Society of America, Albuquerque, NM, 1999, pp. 345–355.

[12]Jordan, J. D., Watkins, A. N., Weaver, W. L., Dale, G. A., and Navarra, K. R., "Sol-Gel-Based Pressure-Sensitive Paint Development," AIAA Paper 99-0566, Jan. 1999.

[13]Upchurch, B. T., Oglesby, D. M., and West, J. P., "New PSP Developments at NASA Langley Research Center–Low Temperature PSP," *Proceedings of the 6th Annual Pressure Sensitive Paint Workshop*, The Boeing Company, Seattle, WA, 1998, pp. 10-1–10-24.

[14]Sakaue, H., and Sullivan, J. P., "Fast Response Time Characteristics of Anodized Aluminum Pressure Sensitive Paint," AIAA Paper 2000-0506, Jan. 2000.

[15]Teduka, N., Kameda, M., Amao, Y., and Asai, K., "Experimental Investigation on Time Response of Pressure-Sensitive Paint," *Proceedings of the 31st Japan Society of Aeronautics and Space Sciences (JSASS) Annual Meeting*, Japan Society of Aeronautics and Space Sciences, Tokyo, Japan, 2000, pp. 218–221 (in Japanese).

[16]Nakakita, K., Yamazaki, T., Asai, K., Teduka, N., Fuji, A., and Kameda, M., "Pressure-Sensitive Paint Measurement in a Hypersonic Shock Tunnel," AIAA Paper 2000-2523, June 2000.

[17]Masuda, T., Isobe, E., and Higashimura, T., "Poly [1-(trimethylsilyl)-1-propyne]: A New High Polymer Synthesized with Transition-Metal Catalysts and Characterized by Extremely High Gas Permeability," *Journal of the American Chemical Society*, Vol. 105, No. 25, 1983, pp. 7473, 7474.

[18]Asai, K., Okura, I., and Nishide, H., "Highly Functional Pressure-Sensitive Paint and Oxygen Sensor," Patent Pending, No. 2000-61625, March 2000, Japan.